The Meteoritical Society

Meteoritics & Planetary Science 44, Nr 4, 521–530 (2009)
Abstract available online at http://meteoritics.org

Cooling rates of porphyritic olivine chondrules in the Semarkona (LL3.00) ordinary chondrite: A model for diffusional equilibration of olivine during fractional crystallization

M. MIYAMOTO[1*], T. MIKOUCHI[1], and R. H. JONES[2]

[1]Space and Planetary Science, Graduate School of Science, University of Tokyo, Hongo, Tokyo 113-0033, Japan
[2]Department of Earth and Planetary Sciences, University of New Mexico, Albuquerque, New Mexico 87131, USA
[*]Corresponding author. E-mail: miyamoto@eps.s.u-tokyo.ac.jp

(Received 04 May 2008; revision accepted 14 December 2008)

Abstract–Cooling rates of chondrules provide important constraints on the formation process of chondrite components at high temperatures. Although many dynamic crystallization experiments have been performed to obtain the cooling rate of chondrules, these only provide a possible range of cooling rates, rather than providing actual measured values from natural chondrules. We have developed a new model to calculate chondrule cooling rates by using the Fe-Mg chemical zoning profile of olivine, considering diffusional modification of zoning profiles as crystals grow by fractional crystallization from a chondrule melt. The model was successfully verified by reproducing the Fe-Mg zoning profiles obtained in dynamic crystallization experiments on analogs for type II chondrules in Semarkona. We applied the model to calculating cooling rates for olivine grains of type II porphyritic olivine chondrules in the Semarkona (LL3.00) ordinary chondrite. Calculated cooling rates show a wide range from 0.7 °C/h to 2400 °C/h and are broadly consistent with those obtained by dynamic crystallization experiments (10–1000 °C/h). Variations in cooling rates in individual chondrules can be attributed to the fact that we modeled grains with different core Fa compositions that are more Fe-rich either because of sectioning effects or because of delayed nucleation. Variations in cooling rates among chondrules suggest that each chondrule formed in different conditions, for example in regions with varying gas density, and assembled in the Semarkona parent body after chondrule formation.

INTRODUCTION

Chondrules, the most abundant component of chondrites, are generally considered to have formed from essentially molten droplets, during rapid cooling from a high temperature of around 1500 °C (e.g., Hewins 1988; Connolly et al. 2006). They contain information on the early stages of solar system formation: for example, cooling rates of chondrules give constraints on the formation processes of chondrite components in the high temperature range. Although many dynamic crystallization experiments have been performed to obtain the cooling rate of chondrules (e.g., Tsuchiyama et al. 1980; Hewins 1988; Hewins et al. 2005), experimental results only show possible ranges of cooling rates at which chondrules form, rather than the actual cooling rate. The Semarkona LL ordinary chondrite is one of the most primitive ordinary chondrites that suffered the least amount of (secondary) thermal metamorphism, and is classified as LL3.00 (Wasson 1993; Grossman and Brearley 2005). It contains many sharply defined chondrules that have clear chemical zoning in olivine. This means we can potentially use zoning profiles in chondrules in this chondrite to determine the actual cooling rates that the chondrules experienced.

Minerals often show chemical zoning that provides information on their thermal history such as cooling, reheating and annealing of terrestrial rocks or extraterrestrial materials (meteorites and lunar rocks, etc.). Because chemical zoning is mainly controlled by atomic partition and atomic diffusion, it enables us to obtain the cooling rate (or burial depth) by analyzing it on the basis of diffusion calculations under the appropriate boundary conditions. Chemical zoning caused by diffusional modification alone (i.e., in the absence of primary igneous zoning) can be applied to calculating the cooling rate or burial depth, by fitting the zoning profile calculated by solving the diffusion equation to the observed zoning profile (e.g., Miyamoto et al. 1986). Although we have previously reported the cooling rate (or burial depth) of many meteorites on the basis of chemical zoning profiles of olivine

or pyroxene (e.g., Miyamoto et al. 1986; Miyamoto and Takeda 1994), these model calculations are based on the assumption that diffusional modification occurred after crystal growth finished. We did not consider diffusional modification during crystal growth at the initial high-temperature formation. In other words, we have only considered diffusional modification starting from the profile established by fractional crystallization after crystal growth ceased, or from an assumed initial zoning profile.

Olivine in type II (FeO-rich) porphyritic olivine chondrules in Semarkona preserves clear Fe-Mg zoning that formed basically by fractional crystallization during the early high-temperature stage of formation (e.g., Jones 1990). The profile calculated by using a closed-system fractional crystallization model, however, shows a subtle mismatch to the observed zoning profile (e.g., Jones 1990; Miyamoto et al. 1998). This mismatch probably means that the primary zoning profile was altered by diffusional modification during the cooling history, including the crystal growth period. In order to model this behavior, we have developed a new model to calculate the cooling rate by using the Fe-Mg chemical zoning profile of olivine, considering diffusional modification during crystal growth (Miyamoto et al. 1999). We have conducted a verification of the new model by using experimentally produced Fe-Mg zoning of olivine formed at a range of cooling rates (Jones and Lofgren 1993). After successful verification, we have applied our model to calculating the cooling rate of euhedral olivines with normal Fe-Mg zoning in several type II porphyritic olivine chondrules in the Semarkona chondrite.

SAMPLES AND EXPERIMENTS

We used a thin section of Semarkona that was kindly supplied by Dr. G. MacPherson. Detailed descriptions of Semarkona chondrules are given by Jones (1990, 1996).

Olivine grains were selected on the basis of backscattered electron images (BEI). Measurements of compositional profiles were made by making spot analyses every one to three micrometers by electron microprobe (JEOL, JCXA-733) at the Ocean Research Institute, University of Tokyo. We estimated the crystallographic axis on the basis of the shape and cleavage of olivine, and measured the zoning profile along the direction as near the *c* axis as possible, because we use the Fe-Mg diffusion coefficient in the *c* direction. For electron microprobe analysis, the acceleration voltage was 15 kV and beam current was 24 nA on a Faraday cage. We analyzed 11 major elements (Si, Mg, Fe, Ca, Na, K, Mn, Al, Ti, Cr, and Ni). Counting times at peak wavelengths were 30 s. The background intensity of each element was counted at both sides of the peak wavelength. We measured 70 zoning profiles of olivines in 17 type II porphyritic olivine chondrules in the thin section.

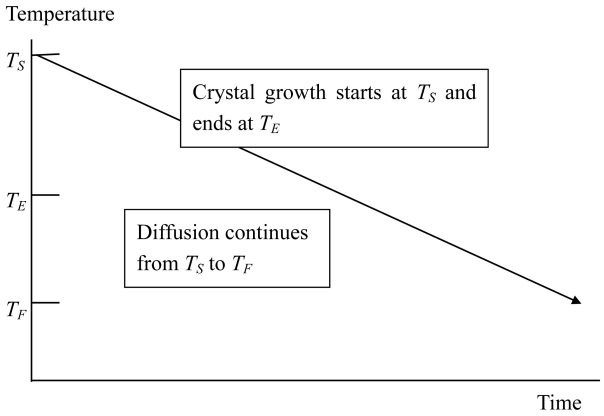

Fig. 1. Schematic diagram of cooling history. The cooling rate is linear. Olivine crystallization begins at T_S, and continues to T_E. In the interval T_E to T_F, zoning in olivine continues to be modified by diffusion.

CALCULATION PROCEDURES

The outline of calculation procedures is as follows. The olivine crystal grows as temperature decreases. Fe-Mg zoning forms by closed-system fractional crystallization as the olivine crystal grows. Fe-Mg diffusion takes place in the growing olivine crystal. By simulating the above processes, we compute the zoning profile and determine the cooling rate by selecting the profile that provides the best fit to the observed one.

Cooling Model

A schematic cooling history is shown in Fig. 1. Crystallization of olivine starts at temperature T_S and ends at temperature T_E as temperature decreases. For the cooling rate calculation, we assume that cooling is linear (continuous) from starting temperature (T_S) to closure temperature (T_F) at which Fe-Mg interdiffusion essentially ceases considering the cooling rate. T_F is lower than ending temperature (T_E). Diffusional modification also starts at T_S, which is starting time of crystallization, and ends at closure temperature (T_F). As the crystal grows, Fe-Mg zoning forms in accordance with the Rayleigh equation for closed-system fractional crystallization, and diffusional modification takes place during ongoing olivine crystal growth.

Olivine Crystal Growth

In this model, we assume that the olivine crystal is a sphere, and that olivine crystal growth is parabolic (e.g., Elwell and Scheel 1975) during the formation of chondrule at high temperature:

$$\frac{dR}{dt} \propto \frac{1}{R} \tag{1}$$

where R is the radius of crystal and t is time. The proportionality constant is determined by the size of the olivine grain and cooling rate (i.e., the growth rate is a function of the size of the olivine grain and cooling time).

Fractional Crystallization

As was pointed out by Jones (1990), Fe-Mg zoning in Semarkona olivine basically formed by fractional crystallization. We calculated an Fe-Mg zoning profile (primary zoning profile) by using the Rayleigh equation for closed-system fractional crystallization (e.g., Jones 1990). The equation is

$$\frac{C_L}{C_0} = F^{K_D - 1} \quad (2)$$

where C_0 and C_L are the initial concentration in the bulk liquid and the concentration in the observed liquid, respectively. K_D is the distribution coefficient, and F is the fraction of liquid remaining. We used the distribution coefficient (partition coefficient) for Fe/Mg of 0.30 (e.g., Stolper 1977; Beattie 1993). As the olivine crystal grows based on Equation 1, with decreasing temperature, the Fe-Mg profile is calculated in accordance with the Rayleigh equation.

Fe-Mg Diffusion

During the formation of the Fe-Mg profile according to Equation 2 during olivine crystal growth, we calculate diffusional modification by solving the diffusion equation. It is assumed that the compositional gradient of the Fa component (=100 × Fe/(Mg + Fe), mol%) of olivine is controlled by Fe-Mg interatomic diffusion (e.g., Miyamoto et al. 1986).

The diffusion equation was numerically solved by using finite difference approximation in spherical coordinates, assuming spherical geometry for the olivine grain:

$$\frac{\partial C}{\partial t} = \frac{1}{r^2}\left\{\frac{\partial}{\partial r}\left(r^2 D \frac{\partial C}{\partial r}\right)\right\} \quad (3)$$

where C, r, and t are the Fa component, position in spherical coordinates, and time, respectively.

The initial condition is

$$C(r, 0) = C_I(r) \quad (4)$$

where C_I is an initial concentration profile. The initial profile for the diffusion equation is the profile obtained by fractional crystallization for a certain size of olivine at a certain temperature. Diffusional modification is calculated progressively as the olivine crystal grows.

Boundary conditions are

$$\frac{\partial C(0, t)}{\partial r} = 0 \quad (5)$$

$$C(R, t) = C_B \quad (6)$$

where position R is at the interface between olivine and the melt, that is, the radius of the olivine crystal as it grows. C_B is the concentration at the grain boundary with the melt, that is, the concentration of the edge of olivine crystal. The boundary condition at the rim of olivine during the diffusional calculation is determined by the Rayleigh equation. R and C_B change with the size of olivine.

Cooling is assumed to be linear (continuous) from the starting temperature T_S to the final temperature T_F:

$$T = T_S - at \quad (7)$$

where a is the cooling rate and t is time. This means that cooling rates determined in our calculations are average cooling rates throughout the cooling period.

Estimation of T_S and T_E

We estimated T_S and T_E by using MELTS under the option of "equilibrium" or "fractionate solids" (Ghiorso and Sack 1995) for the bulk chemical composition of a typical Semarkona type II chondrule (Jones 1990). Olivine is a major liquidus phase for this composition. In the equilibrium model, the amount of olivine increases down to 1270 °C and then decreases gradually by a reaction between olivine and melt to form orthopyroxene at lower temperatures. We estimated T_S as the temperature at which olivine having the core Fa component crystallizes, using the fractionate solids option. We also estimated T_E at which olivine having the rim Fa component crystallizes, using the fractionate solids option. However, if T_E estimated using the fractionate solids option is higher than 1270 °C, then T_E is set to 1270 °C, because we cannot exclude the possibility that the olivine crystal grows down to 1270 °C at which olivine continues to grow under the equilibrium condition, if orthopyroxene crystallization is suppressed. We employed a closure temperature (T_F) of 900 °C at which Fe-Mg interdiffusion essentially ceases. This temperature was based on a consideration of the cooling rate, and the appropriate value of the diffusion coefficient taking into account the oxygen fugacity reported by Brett and Sato (1984) for Semarkona.

Diffusion Model: Determination of Unknown Parameters

With the model set up as described above, there are three unknown parameters to be determined: cooling rate, initial concentration for fractional crystallization (C_0), and fraction of liquid remaining (F). We determined these parameters by employing the non-linear least squares method (Simplex method; Nelder and Mead 1965) to fit the computed zoning profile to the observed zoning. The calculation procedures are as follows:

1. Determination of T_S and T_E by using MELTS.

2. Estimation of initial values for the three unknown parameters (i.e., the cooling rate, and C_0 and F in Equation 2.
3. Determination of the proportionality constant in Equation 1 from the given cooling rate and the size of olivine crystal now observed.
4. For a given short time, calculation of the size of olivine crystal growth by Equation 1.
5. Calculation of the zoning profile for the small olivine crystal by using the Rayleigh equation (Equation 2) for a given short time.
6. By employing this calculated zoning profile as the initial profile for Equation 4 and the fixed boundary conditions of Equation 6 determined by the distribution coefficient between olivine and the melt, we obtain the zoning profile after the short time elapsed.
7. Procedures 4–6 are repeated until the olivine grain has grown to the size now observed, as time proceeds and temperature decreases. At each step, a new node is added to the finite difference mesh.
8. Calculation of the residuals by comparing the calculated profile with observed profile.
9. Determination of the three unknown parameters to minimize the residuals by the Simplex method by repeating procedures 3–7.

Because the non-linear least squares method sometimes converges on some local minima of the function to be minimized, we performed non-linear least squares for several different initial values for unknown parameters and took the values of the parameters that give the minimum residuals.

Diffusion Coefficient

In our model, we assume that the compositional gradient of the Fa component of olivine is controlled by Fe-Mg interatomic diffusion. The results are thus strongly dependent on the value of the Fe-Mg interdiffusion coefficient used in the calculations (D_{Fe}). Although several expressions of the Fe-Mg interdiffusion coefficient in olivine have been reported (e.g., Buening and Buseck 1973; Misener 1974; Nakamura and Schmalzried 1984; Jurewicz and Watson 1988; Chakraborty 1997), there are about two orders of magnitude difference among these values (see Fig. 1 in Miyamoto et al. 2002). This difference gives about two orders of magnitude difference in the calculated cooling rate. Miyamoto et al. (2002) evaluated the Fe-Mg interdiffusion coefficient by examining Fe-Mg chemical zoning produced experimentally and concluded that the profile calculated by the Fe-Mg diffusion coefficient reported by Misener (1974), with consideration of the effect of oxygen-fugacity included, gives the best fit to the observed zoning profile.

The expression of the Fe-Mg interdiffusion coefficient by Misener (1974), for olivine parallel to the *c* axis, is

$$D_{Fe} = 10^{-2}(0.41 + 0.0112C_{Fe}) \exp[(-58.88 + 0.0905C_{Fe})/RT], \quad 900\ ^\circ\text{C} \le T \le 1100\ ^\circ\text{C} \tag{8}$$

where D_{Fe} is the Fe-Mg interdiffusion coefficient in cm^2/s, C_{Fe} is the Fa component in mol%, R is the gas constant in kcal mol^{-1} K^{-1} and T is temperature in K. Misener (1974) did not report oxygen-fugacity (fO_2) dependence, because his experiments are performed under the QFM (quartz-fayalite-magnetite) buffer of oxygen fugacity. Buening and Buseck (1973) demonstrated the dependence of the Fe-Mg interdiffusion coefficient in olivine on temperature, composition and oxygen fugacity. Miyamoto et al. (1986) and Miyamoto et al. (2002) extrapolated the D_{Fe} reported by Misener (1974) by using an equation for variation with oxygen fugacity similar to that of Buening and Buseck (1973). This extrapolation enables us to employ the Fe-Mg diffusion coefficient of Misener (1974) under any oxygen-fugacity conditions. The D_{Fe} of olivine extrapolated by Miyamoto et al. (2002) is

$$\begin{aligned} D_{Fe} &= (fO_2)^{1/6} \exp[\ln(0.0041 + 0.000112C_{Fe}) - 3.4538] \\ &\quad \exp[(-39.27 + 0.0905C_{Fe})/RT] \\ &= 0.03163 \times 10^{-2} (fO_2)^{1/6}(0.41 + 0.0112C_{Fe}) \exp[(-39.27 \\ &\quad + 0.0905C_{Fe})/RT], \ 900\ ^\circ\text{C} \le T \le 1100\ ^\circ\text{C} \end{aligned} \tag{9}$$

where fO_2 is the oxygen fugacity in atm. Although this equation strictly applies to the temperature range 900–1100 °C, extrapolation of the equation to higher temperature ranges is not problematic, because there is not likely to be a change in the activation energy of diffusion at high temperatures.

We calculate the temperature dependence of the oxygen fugacity by using the fO_2-temperature relation reported by Brett and Sato (1984) for Semarkona:

$$\log(fO_2) = 3.6 - 24400/T \tag{10}$$

The diffusion coefficient in the *c* direction was used, because diffusion in this direction is the fastest among the three crystallographic directions, and diffusional modification tends to be dominated by the largest diffusion coefficient.

VERIFICATION

Chondrule Olivine

Jones and Lofgren (1993) experimentally produced porphyritic olivine textures by dynamic crystallization of a bulk chemical composition similar to a type II porphyritic chondrule of Semarkona. They reported Fe-Mg zoning profiles of olivine from experiments that were continuously (linearly) cooled at 2 °C/h from 1525 °C to 985 °C, 5 °C/h from 1550 °C to 1015 °C, and 100 °C/h from 1525 °C to 1200 °C. We used these experimentally produced profiles for

verification of our model, that is, we calculated the cooling rate by using our model to obtain the best-fit profile to the experimentally produced zoning profile. We estimated both the temperature (T_S) at which olivine crystallization begins and temperature (T_E) at which olivine crystallization terminates by using MELTS (Ghiorso and Sack 1995) for the bulk chemical composition of the experimental starting material. For the 2 °C/h, 5 °C/h, and 100 °C/h experiments, values of T_S are 1500 °C, 1450 °C, and 1410 °C, respectively, and T_E is 1270 °C in all cases. T_S is dependent on the core Fa component. T_F is the same as the temperature at which the experiment finished. Because the experiments were carried out at $\log fO_2 = IW-0.5$, we used this oxygen fugacity in the model verification.

Figure 2 shows the results of verification. Open circles show the zoning profiles produced by dynamic crystallization experiments reported by Jones and Lofgren (1993) and solid curves show the calculated profiles. The best-fit cooling rates obtained by our model calculations are 2.5 °C/h for the 2 °C/h cooling experiment, 6.2 °C/h for the 5 °C/h cooling experiment and 124 °C/h for the 100 °C/h cooling experiment. The calculated zoning profiles are in good agreement with the experimentally produced profiles. These results mean that the Fe-Mg interdiffusion coefficient reported by Misener (1974) with oxygen-fugacity dependence (Miyamoto et al. 2002) is relatively accurate and that our model for calculating the cooling rate on the basis of Fe-Mg zoning considering the crystal growth gives a good estimation of the cooling rate.

Miyamoto et al. (2006) also performed verification of our model for zoning profiles experimentally produced by dynamic crystallization of martian and lunar meteorite compositions. Although the bulk chemical compositions of these meteorites are different from the Semarkona composition, the estimated cooling rates are in good agreement with experimental values. These results mean that our model can be of use for a wide variation of chemical compositions. The computer program of our model written by Fortran can be used on Microsoft Windows.

RESULTS AND DISCUSSION

Figure 3 shows examples of the fitting results for olivines in different type II porphyritic olivine chondrules. Open circles show zoning profiles measured by electron microprobe and solid curves show the calculated profiles. Table 1 summarizes the observed and calculated results for olivine grains in different chondrules. The calculated cooling rates show a wide range, from 0.7 °C/h to 2400 °C/h, and are different among chondrules. This result suggests that each chondrule formed in different environmental conditions and assembled in Semarkona after chondrule formation. The cooling rates for different olivines in the same chondrule have roughly similar values (CH1, CH5, CH6, CH10, and CH16 in Table 1). These results indicate that olivine grains in the same chondrule formed in similar environmental conditions. The cooling rates for many olivine grains in CH5 vary from 7.3 °C/h to 23 °C/h and the average value is 16 °C/h with standard deviation of 6 °C/h, giving an estimate of our model. This level of error is reasonable considering the heterogeneous distribution of crystals in the melt. Representative zoning profiles for several olivines in CH5 are shown in Fig. 3 (panels c, d, and e). The zoning profile for a different direction in the same olivine grain gives a similar cooling rate (L47, L48, and L70 in Table 1). The dashed curve in Fig. 3c shows the profile calculated by the Rayleigh equation without diffusional modification. The difference between the dashed and solid curves is caused by Fe-Mg diffusion.

We determined the sensitivity of our model to the calculated parameters T_S and T_E, by calculating cooling rates for the L17 zoning profile with a range of values for T_S and T_E (Table 2). The difference in T_S does not significantly affect the calculated cooling rate, i.e., the effect of supercooling of T_S for the cooling rate calculation is negligible for our model. However, a change of T_E does affect the result significantly: 100 °C of difference in T_E results in a factor of 3–4 times difference in the cooling rate.

The calculated Fa component of the initial concentration for fractional crystallization (C_0) is usually smaller than the core composition of the corresponding observed profile (Table 1), because the core Fa component now observed increases by Fe-Mg diffusion during cooling. Because the temperature T_S is determined by the Fa component at the onset of olivine crystallization (that is, C_0), as discussed above, we determined T_S that is consistent with C_0 by iteration. Although the difference in T_S does not significantly affect the calculated cooling rate, we performed this iteration process.

For the measured zoning profiles, we selected olivine grains with the most Mg-rich core compositions or largest sizes in a given chondrule. These properties are most likely to represent earlier nucleation and cutting near the center of the crystal, compared with grains that have more Fe-rich core compositions. We computed the cooling rate for several olivine grains in CH5 to compare the results for different grains (Table 1). The difference in the core Fa component of olivines in CH5 is partly due to the cutting effect (sections at different distances from the centers of olivine crystals), and also partly due to the time of nucleation of the crystal. We used the T_S determined from the core Fa component of each olivine by using the MELTS program. The T_S is different varies with the core Fa component, because the core Fa component increases as the temperature decreases. This may partly relieve the effects of cutting and the time of nucleation, because olivine having more Fe-rich core compositions may crystallize at a lower temperature. In order to check these effects, we showed the results for olivines having different core compositions for CH5 and CH6 (Table 1). The

Table 1. Calculated cooling rate for olivines in type II porphyritic olivine chondrules.

Chondrule no.	Line no.	Olivine no.	Obs. core Fa	Obs. rim Fa	Interval (μm)	Length (μm)	T_S (°C)	T_E (°C)	Initial Fa	Residual melt (%)	Cooling rate (°C/h)	Average for chondrule	Remarks
CH1	L1	OL1	13.5	26.7	2	38	1440	1270	13.6	31	1600	1350	
	L2	OL2	14.0	37.0	2	36	1450	1225	13.7	15	1100		Fig. 3a
CH2	L4	OL3	12.9	24.6	3	48	1450	1270	12.3	29	13	13	
CH3	L5	OL4	7.9	16.9	2	34	1600	1270	7.7	32	1900	2150	
	L6	OL5	9.6	23.5	2	28	1560	1270	9.4	21	2400		Fig. 3b
CH4	L7	OL6	17.4	36.5	3	21	1425	1230	15.1	21	50	50	
CH5	L10	OL7	10.5	28.2	2	34	1515	1270	9.0	13	23	15.6	σ = 6.0
	L17	OL8	9.4	32.4	1.5	78	1600	1260	8.4	9.4	13		Fig. 3c
	L18	OL9	9.2	25.5	1.5	64.5	1580	1270	8.3	13	23		Fig. 3d
	L19	OL10	9.5	29.9	1.5	34.5	1615	1270	7.0	7.5	21		
	L22	OL11	18.9	34.0	1.5	25.5	1420	1240	15.3	31	12		
	L23	OL12	13.2	27.9	1.5	51	1500	1270	10.9	19	7.3		Fig. 3e
	L47	OL8	9.0	34.8	1.5	67.5	1615	1240	7.4	6.3	8.1		L17 + 45°
	L48	OL9	9.0	25.9	1.5	63	1550	1270	7.9	13	17		L18 – 30°
CH6	L13	OL13	14.5	33.6	2	36	1485	1245	11.9	27	11	7.8	
	L20	OL14	9.4	27.7	1.5	64.5	1615	1270	7.1	11	4.4		Fig. 3f
CH7	L14	OL15	6.5	11.5	3	87	1630	1270	6.3	46	120	120	Fig. 3g
CH8	L29	OL16	8.8	25.1	1.5	85.5	1625	1270	7.0	12	3.8	3.8	
CH10	L60	OL17	9.6	14.6	3	93	1635	1270	6.3	26	0.9	0.8	Fig. 3h
	L61	OL18	8.2	13.1	3	189	1615	1270	7.2	41	0.7		
CH16	L69	OL19	11.0	14.3	2	36	1535	1270	9.5	49	11	11.0	
	L70	OL19	10.8	14.6	2	40	1535	1270	9.6	48	11		L69 + 180°
CH17	L71	OL20	14.0	18.6	2	34	1450	1270	14.3	65	1100	1100	

Table 2. Change of the cooling rate with T_S and T_E.

	Constant T_S = 1600 °C								
T_E (°C)	1350	1325	1300	1275	1260	1225	1200	1175	1150
Cooling rate (°C/h)	33.4	25.5	19	14.2	12.7	7.58	5.48	3.91	2.77
	Constant T_E = 1260 °C								
T_S (°C)	1600	1550	1500	1450					
Cooling rate (°C/h)	12.7	11.4	11	10.7					

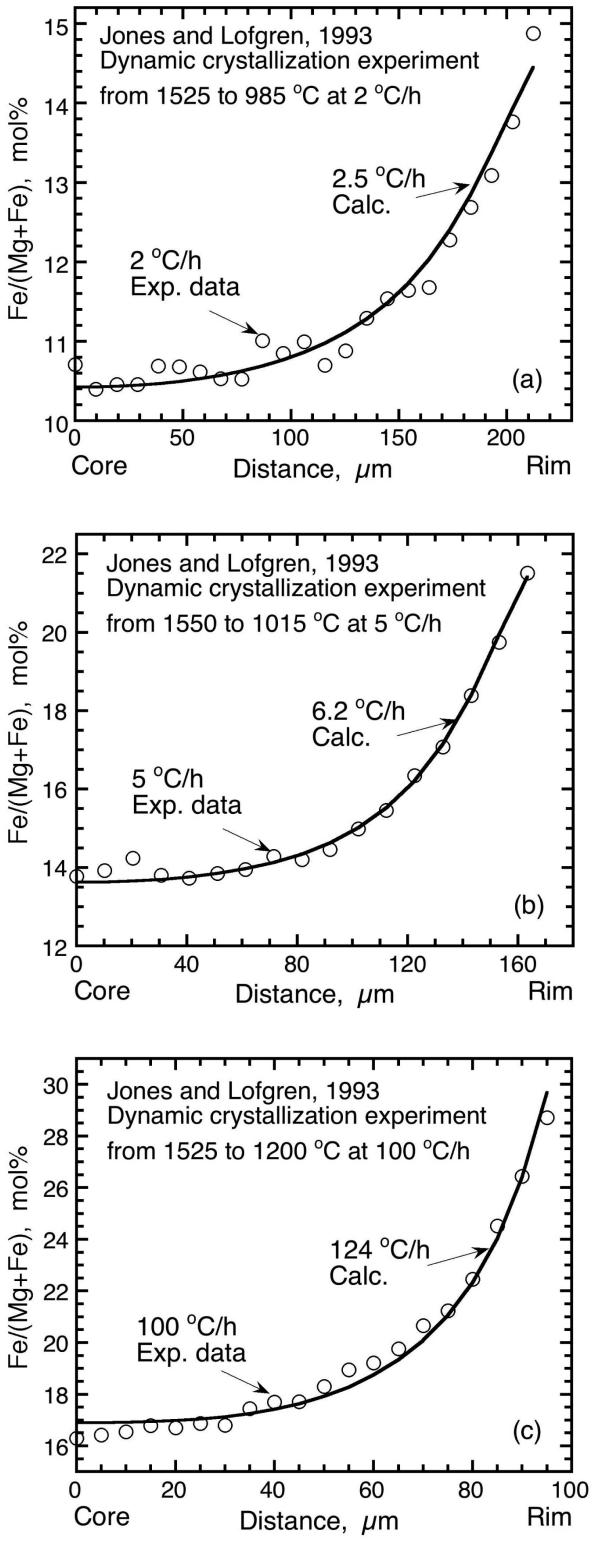

Fig. 2. Comparison of the calculated zoning profiles (solid curves) with the observed zoning profiles (open circles) produced by dynamic crystallization experiments by Jones and Lofgren (1993). (a) 2 °C/h, (b) 5 °C/h, and (c) 100 °C/h cooling experiments. Solid curves show the best-fit to the observed profiles and numbers show both the best-fit cooling rates and experimental cooling rates.

differences in cooling rates determined for grains of different core composition, e.g., $Fa_{9.2}$ (L18) and Fa_{19} (L22), 23 and 12 °C/h, respectively, are comparable to the range of cooling rates determined for similar core compositions e.g., $Fa_{9.4}$ (L17) and $Fa_{9.2}$ (L18), 13 and 23 °C/h, respectively.

The calculated values of the fraction of liquid remaining (F) range from 6% to 49% (Table 1). In comparison, observed values of the amount of melt reported by Jones (1990) for Semarkona chondrules range from 15 to 37%. Our calculated results are broadly consistent with the observed values. Since we only used a single, generalized bulk composition for all our calculations, we consider this to be reasonable agreement. The fraction of liquid remaining calculated for different olivine grains in the same chondrule shows a wide range: for example, from 6% to 31 vol% for CH5. The high value of 31 vol% is for the calculation that uses a high core Fa content (Fa_{19}), and this is consistent with a short crystallization interval. For grains with (measured and calculated) core Fa values <10 mole%, the range of values for F is much more limited, 6 to 13 vol%. In addition, the same olivine grain in the same chondrule shows a similar value (L17 and L47, L18 and L48, L69, and L70). This illustrates the variability of the results based on the exact input parameters (core and rim olivine composition, length of zoning profile) used for each calculation.

According to the summary by Hewins et al. (2005), porphyritic olivine chondrules can be experimentally reproduced at linear cooling rates of 10–1000 °C/h. Cooling rates as low as 0.1 °C/h, determined from exsolution features in pyroxene (Weinbruch et al. 1998), are relevant to a lower temperature range than the crystallization interval (1000 to 1200 °C), and indicate that the true cooling rate curve for chondrules is most likely non-linear. Our calculation results of cooling rates in the range 1 to 2400 °C/h are broadly consistent with the experimental results. Although higher cooling rates in chondrules are typically associated with textures indicative of high growth rates, e.g., barred and excentroradial textures, textures are also strongly controlled by factors such as the presence of seed nuclei (e.g., Lofgren 1996; Hewins et al. 2005). We applied our model only to normally zoned euhedral olivines: further studies are needed to obtain the cooling rates for different textures of olivine such as skeletal or barred textures. Our results show that some calculations give cooling rates as slow as 1 °C/h, slower than the lower limit of the cooling rate (10 °C/h) indicated by dynamic crystallization experiments. Our results suggest that type II porphyritic olivine chondrules actually formed with a wide variety of cooling rates. Our results are important, because experimental results only show the possible range of cooling rates at which porphyritic olivine chondrules form, whereas we have shown a measured range of values.

Wasson and Rubin (2003) and Wasson (2004) argued for very rapid cooling rates of 10^3 K/s for chondrules, based on observations of thin overgrowths on relict olivine grains. This

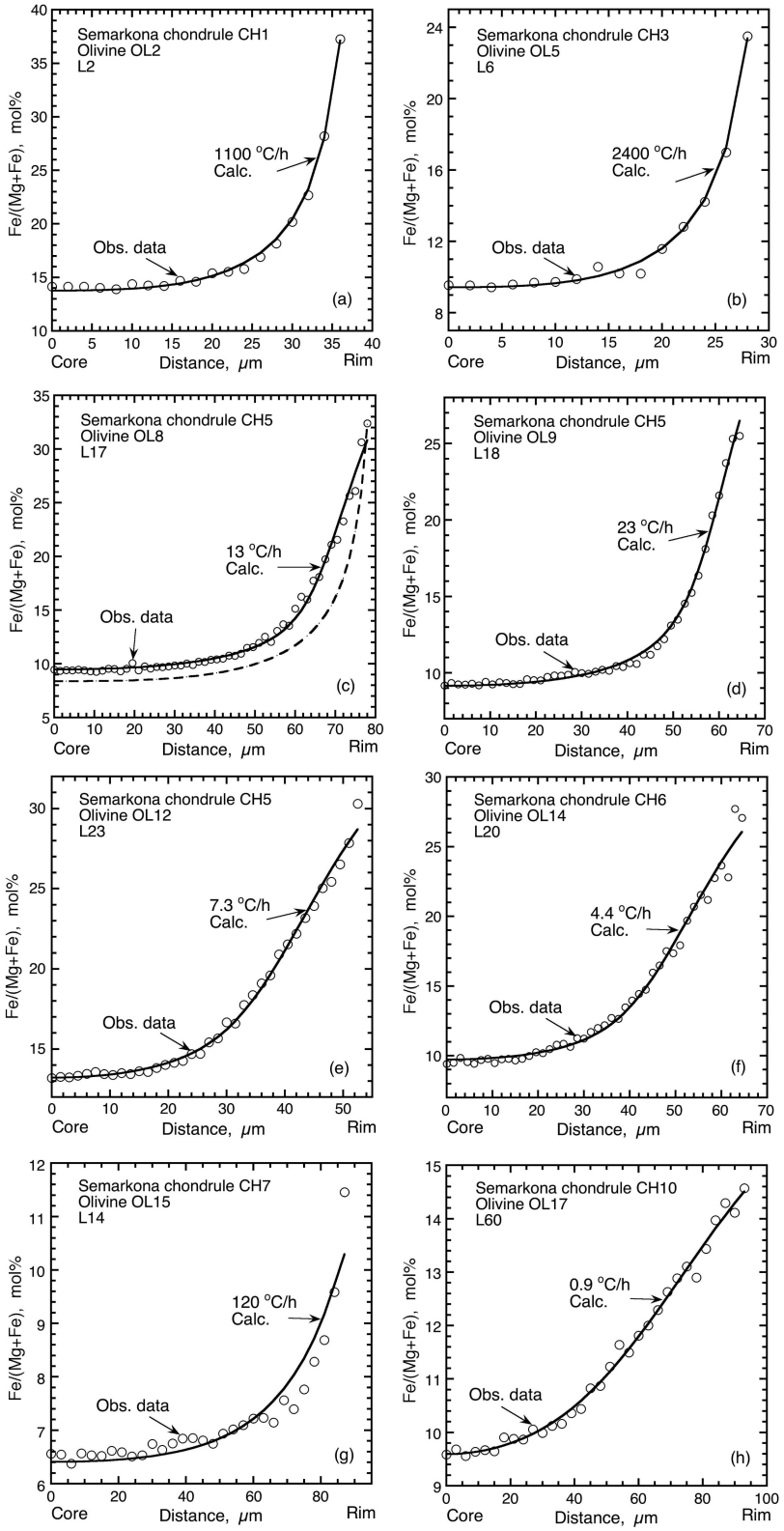

Fig. 3. Calculated zoning profiles (solid curves) and observed zoning profiles (open circles) for the Fa (= 100 × Fe/(Mg+Fe), mol%) component of olivines in type II porphyritic olivine chondrules of Semarkona (LL3.00). (a)–(h) show different olivines in chondrules; c)–(e) are all from chondrule 5. Solid curves show the best-fit to the observed profiles and numbers on curves show the best-fit cooling rates calculated by our model. Dashed curve in (c) shows the profile calculated by the fractional crystallization model without diffusional modification, for comparison. The observed and calculated values for these profiles are summarized in Table 1.

result is about 10^3 times faster than both experimental results (e.g., Hewins 1988) and our calculations. Wasson and Rubin (2003) have argued that in a type II chondrule, the majority of the volume of each olivine crystal is a relict grain, and that only the outer few micrometers of an existing olivine grain grew from the melt during the last chondrule melting event. We have demonstrated clearly that zoning profiles in olivine crystals are strongly consistent with a model in which olivine crystals grow essentially entirely by fractional crystallization, with diffusion occurring within the crystal during the crystallization interval. In addition to the consistency with experimental observations, this provides a robust argument against the very rapid cooling rates proposed by Wasson and Rubin (2003) and Wasson (2004). Additional experimental observations that contradict the very rapid cooling rates are summarized by Hewins et al. (2005).

In our model, we assume linear cooling rates for chondrule olivines. This is most likely a simplification because chondrules are more likely to have experienced non-linear cooling rates (e.g., Hewins et al. 2005). Further work would be required to constrain cooling rates based on a non-linear cooling model. The cooling rates we have determined should be viewed as estimates of the average cooling rate over the 200–300 °C interval relevant to olivine crystallization, and as such are reasonable parameters to compare with cooling rates predicted in chondrule formation models.

The range of cooling rates calculated from our modeling is a plausible range for chondrule formation in the solar nebula. For example, the shock model for chondrule formation proposed by Desch and Connolly (2002) gives cooling rates ranging from 5 to 10,000 °C/h, for gas densities varying from 3×10^{-10} g/cm^3 to 3×10^{-9} g/cm^3 and shock speeds from 6 km/s to 9 km/s. In order to account for a range of cooling rates in similar types of chondrules in the same chondrite, such as we infer for Semarkona, we would need to propose that they are derived from a region of the solar nebula with local heterogeneity in gas density. This could be either a result of changes in density with depth in a dense chondrule formation region, or gas density could vary less systematically as a result of turbulence. Chondrules with varying cooling rates could have been mixed by turbulence and settling after formation. Because these conditions are related to the frequency of shock events, heterogeneity in the chondrule formation region, and the magnitude of turbulence, further observational and theoretical studies for chondrules are needed to clarify the conditions of chondrule formation.

CONCLUSIONS

The conclusions reached in the present study are the following:

1. We developed a new model to calculate the cooling rate of olivine in porphyritic olivine chondrules, by using the Fe-Mg chemical zoning profile of olivine and considering diffusional modification during crystal growth.
2. Our model was successfully verified by reproducing the Fe-Mg zoning profiles obtained in dynamic crystallization experiments on analogs for type II chondrules in Semarkona.
3. Calculated linear cooling rates for olivine grains in Semarkona chondrules are broadly consistent with those determined in dynamic crystallization experiments (10–1000 °C/h), although they span a larger range, 1–2400 °C/h. According to experiments, cooling rates >1000 °C/h are typically characterized by textures indicative of high growth rates, but the chondrules for which we calculate fast cooling rates are all porphyritic with euhedral olivine crystals.
4. The calculated cooling rates are different among individual chondrules. This result suggests that individual chondrules formed under different conditions, for example in regions of different gas densities in a shock-wave model for chondrule formation, and were subsequently mixed after chondrule formation, before assembly into the Semarkona parent body.

Acknowledgments—We thank G. MacPherson for the Semarkona thin section. We also thank K. Ozawa, M. Kimura, and H. Hiyagon for discussion. Helpful comments from R. H. Hewins, N. L. Chabot, and two anonymous reviewers greatly improved the manuscript.

Editorial Handling—Dr. Nancy Chabot

REFERENCES

Beattie P. 1993. Olivine-melt and orthopyroxene-melt equilibria. *Contribution to Mineralogy and Petrology* 115:102–111.

Brett R. and Sato M. 1984. Intrinsic oxygen fugacity measurements on seven chondrites, a pallasite, and a tektite and the redox state of meteorite parent bodies. *Geochimica et Cosmochimica Acta* 48:111–120.

Buening D. K. and Buseck P. R. 1973. Fe-Mg lattice diffusion in olivine. *Journal of Geophysical Research* 78:6852–6862.

Chakraborty S. 1997. Rates and mechanisms of Fe-Mg interdiffusion in olivine at 980 °C–1300 °C. *Journal of Geophysical Research* 102:12317–12331.

Connolly H. C. Jr., Desch S. J., Ash R. D., and Jones R. H. 2006. Transient heating events in the protoplanetary nebula. In *Meteorites and the early solar system II*, edited by Lauretta D. and McSween H. Y. Jr. Tucson: The University of Arizona Press. pp. 383–397.

Desch S. J. and Connolly H. C. Jr. 2002. A model of the thermal processing of particles in solar nebula shocks: Application to the cooling rates of chondrules. *Meteoritics & Planetary Science* 37: 183–207.

Elwell D. and Scheel H. J. 1975. *Crystal growth from high-temperature solutions*. London: Academic Press Inc. 634 p.

Ghiorso M. and Sack R. 1995. Chemical mass transfer in magmatic processes IV. A revised and internally consistent thermodynamic model for the interpolation and extrapolation of liquid-solid

equilibria in magmatic systems at elevated temperatures and pressures. *Contribution to Mineralogy and Petrology* 119:197–212.

Grossman J. N. and Brearley A. J. 2005. The onset of metamorphism in ordinary and carbonaceous chondrites. *Meteoritics & Planetary Science* 40:87–122.

Hewins R. H. 1988. Experimental studies of chondrules. In *Meteorites and the early solar system*, edited by Kerridge J. F. and Matthews M. S. Tucson: The University of Arizona Press. pp. 660–679.

Hewins R. H., Connolly H. C. Jr., Lofgren G. E., and Libourel G. 2005. Experimental constraints on chondrule formation. In *Chondrites and the protoplanetary disk*, edited by Krot A. N., Scott E. R. D., and Reipurth B. ASP Conference Series, vol. 341. San Francisco: Astronomical Society of the Pacific. pp. 286–316.

Jones R. H. 1990. Petrology and mineralogy of Type II, FeO-rich chondrules in Semarkona (LL3.0): Origin by closed-system fractional crystallization with evidence for supercooling. *Geochimica et Cosmochimica Acta* 54:1785–1802.

Jones R. H. 1996. FeO-rich, porphyritic pyroxene chondrules in unequilibrated ordinary chondrites. *Geochimica et Cosmochimica Acta* 60:3115–3138.

Jones R. H. and Lofgren G. E. 1993. A comparison of FeO-rich, porphyritic olivine chondrules in unequilibrated chondrites and experimental analogues. *Meteoritics* 28:213–221.

Jurewicz A. J. G. and Watson E. B. 1988. Cations in olivine, Part 2: Diffusion in olivine xenocrysts, with applications to petrology and mineral physics. *Contribution to Mineralogy and Petrology* 99:186–201.

Lofgren G. E. 1996. A dynamic crystallization model for chondrule melts. In *Chondrules and the protoplanetary disk*, edited by Hewins R. H., Jones R. H., and Scott E. R. D. Cambridge: Cambridge University Press. pp. 187–196.

Misener D. J. 1974. Cationic diffusion in olivine to 1400 °C and 35 kbar. In *Geochemical transport and kinetics*, edited by Hofmann A. W., Giletti B. J., Yoder H. S. Jr., and Yund R. A. Carnegie Institute Washington Publication 634. pp. 117–129.

Miyamoto M. and Takeda H. 1994. Thermal history of lodranites Yamato 74357 and MAC 88177 as inferred from the chemical zoning of pyroxene and olivine. *Journal of Geophysical Research* 99:5669–5677.

Miyamoto M., McKay D. S., McKay G. A., and Duke M. B. 1986. Chemical zoning and homogenization of olivines in ordinary chondrites and implications for thermal histories of chondrules. *Journal of Geophysical Research* 91:12804–12816.

Miyamoto M., Mikouchi T., and Kaiden H. 1998. An analysis of iron-magnesium zoning of olivine in a Semarkona (LL3.0) porphyritic olivine chondrule: Diffusional modification of primary zoning (abstract). *Meteoritics & Planetary Science* 33:A111–A112.

Miyamoto M., Mikouchi T., and Kaiden H. 1999. Diffusional modification of igneous zoning during crystal growth: analysis of Fe-Mg zoning of olivine in Semarkona (LL3.0) porphyritic olivine chondrule (abstract #1323). 30th Lunar and Planetary Science Conference. CD-ROM.

Miyamoto M., Mikouchi T., and Arai T. 2002. Comparison of Fe-Mg interdiffusion coefficients in olivine. *Antarctic Meteorite Research* 15:143–151.

Miyamoto M., Koizumi E., and Mikouchi T. 2006. Verification of a model to calculate cooling rates in olivine by consideration of Fe-Mg diffusion and olivine crystal growth II (abstract #1538). 37th Lunar and Planetary Science Conference. CD-ROM.

Nakamura A. and Schmalzried H. 1984. On the Fe^{2+}-Mg^{2+}-interdiffusion in olivine (II). *Physical Chemistry* 88:140–145.

Nelder J. A. and Mead R. 1965. A simplex-method for function minimization. *Computer Journal* 7:308–313.

Stolper E. 1977. Experimental petrology of eucritic meteorites. *Geochimica et Cosmochimica Acta* 41:587–611.

Tsuchiyama A., Nagahara H., and Kushiro I. 1980. Experimental reproduction of textures of chondrules. *Earth and Planetary Science Letters* 48:155–165.

Wasson J. T. 1993. Constraints on chondrule origins. *Meteoritics* 28:14–28.

Wasson J. T. 2004. Petrographic evidence for rapid heating and cooling during chondrule formation (abstract #9113). Workshop on Chondrules and the Protoplanetary Disk.

Wasson J. T. and Rubin A. E. 2003. Ubiquitous low-FeO relict grains in type II chondrules and limited overgrowths on phenocrysts following the final melting event. *Geochimica et Cosmochimica Acta* 67:2239–2250.

Weinbruch S., Buttner H., Holzheid A., Rosenhauer M., and Hewins R. H. 1998. On the lower limit of chondrule cooling rate: The significance of iron loss in dynamic crystallization experiments. *Meteoritics & Planetary Science* 33:65–74.